Exclusive inelastic final states in $\bar{p}p$ interactions at 49 GeV/c

D. E. Zissa, V. E. Barnes, D. D. Carmony, L. J. Dauwe, J. A. Gaidos, L. J. Gutay, A. T. Laasanen, R. L. McIlwain, and L. K. Rangan

Department of Physics, Purdue University, West Lafayette, Indiana 47907

(Received 8 July 1980)

We have measured the total and subchannel cross sections for the reaction $\bar{p}p \to \bar{p}p\pi^+\pi^-$ at 49 GeV/c. This reaction is dominated by two production mechanisms, diffraction and meson exchange. In addition, we have measured the total cross section for $\bar{p}p \to \bar{p}p2\pi^+2\pi^-$ and compared it to values at other momenta and with the corresponding pp interaction. Within the present statistics, no significant amount of exclusive annihilation is found into two, four, and six charged pions.

I. INTRODUCTION

In this paper we report on an experimental study of exclusive four- and six-prong antiproton-proton interactions:

$$\bar{p}p \to \bar{p}p\pi^+\pi^-, \tag{1}$$

$$\bar{p}p \to \bar{p}p2\pi^+2\pi^- \tag{2}$$

at an incident $\bar{p}$ laboratory momentum of 48.9 ± 0.5 GeV/c.

In Sec. II the procedure for event selections and background and fitting-efficiency studies are given together with cross-section results for reactions (1) and (2).

In Sec. III evidence is presented that suggests reaction (1) is dominated by single diffractive dissociation:

$$\bar{p}p \to \bar{p}N^{*+}, \tag{3a}$$

$$\bar{p}p \to \bar{N}^{*-}p, \tag{3b}$$

where N^{*+} is defined as the $p\pi^+\pi^-$ system with mass <2.5 GeV/c^2. A copious Δ^{++} signal is found in the N^{*+} system. The results for the total cross sections for reaction (3) are compared with results obtained at other momenta with $\bar{p}$ and p beams. From the energy and momentum-transfer dependence of the cross section, the pion rapidity correlations, and the mass distributions it is deduced that reaction (3) is generated via diffractive dissociation. [No low-effective-mass enhancements in $p2\pi$ or $p4\pi$ systems (not shown) have been found in reaction (2).] Also, in Sec. III the following two-body final state is examined:

$$\bar{p} + p \to \bar{\Delta}^{--}(1232) + \Delta^{++}(1232). \tag{4}$$

The energy dependence of the cross section for reaction (4) is compared with other meson-exchange cross sections and with the zero-prong cross section and thus an explanation of the production mechanism is obtained in terms of pion exchange.

We report in Sec. IV on an attempt to find annihilation reactions into two, four, and six charged pions

$$\bar{p}p \to \pi^+\pi^-, \tag{5}$$

$$\bar{p}p \to 2\pi^+2\pi^-, \tag{6}$$

$$\bar{p}p \to 3\pi^+3\pi^-, \tag{7}$$

and compare the results with extrapolations of reactions (5)–(7) at lower energies.

Finally, the results are summarized in Sec. V.

The data sample discussed in this paper was obtained from the 30-in. rapid-cycling bubble chamber exposed to an enriched $\bar{p}$ beam at Fermi National Accelerator Laboratory. The beam production, the beam line, the tagging system, and the hybrid bubble-chamber–proportional-wire-chamber system have been described previously.[1]

All topologies were measured on image-plane scanning and measuring projectors on line to a computer with the TVGP geometrical-reconstruction program. About 45 and 70% of the fast tracks with laboratory momenta p_f in the ranges $15 < p_f < 25$ GeV/c and $p_f > 25$ GeV/c, respectively, were matched with tracks in the four downstream proportional wire chambers. With a successful match 7–10% momentum resolution was achieved. In the set of selected four-constraint fits to reactions (1) and (2) 71% of the tracks above 25 GeV/c were matched. Low-momentum positive particles ($p_{\text{lab}} < 1.33$ GeV/c) were identified as protons or pions by visual estimation of specific track ionization density.

II. EVENT SELECTION, BACKGROUND AND FITTING-EFFICIENCY STUDIES, AND CROSS SECTIONS

Four-constraint fits to hypotheses (1) and (2) were attempted on 2252 four-prong and 1455 six-prong events, respectively. The SQUAW fitting program was modified to require conservation of $\vec{p}$ and $E - \vec{p}\cdot\hat{n}$ where $E, \vec{p}$ denote energy and mo-

mentum and $\hat{n}$ denotes a unit vector along the beam direction. The fiducial volume cuts allowed for at least 20 and 30 cm of track length for secondary tracks from four- and six-prong events, respectively. The χ^2 value of the kinematic fit was required to be less than 30 for both hypotheses as it was previously for the elastic events.[1] Only fits which were consistent with the ionization density scan of slow positive particles ($p_{lab} < 1.33$ GeV/c) were accepted. Also, the fitted events were required to be consistent with scanning information which included comments on π-μ-e decays, kinks, and Dalitz pairs. Strange-particle decays and γ conversions to e^+e^- pairs in the chamber were measured. Where it was determined that they were associated with events that also gave fits to hypotheses (1) and (2), the events were dropped from the samples. From the CP invariance of the interacting $\bar{p}p$ system, it follows that the Feynman-x distribution of particles in the forward c.m. hemisphere is equal to the $|x|$ distribution of antiparticles in the backward hemisphere. To help reduce the background for reaction (1) without losing any significant amount of signal, only those fits were retained which satisfy the following conditions on the Feynman-x values of the outgoing tracks:

$$x(p) < 0.0, \tag{8a}$$

$$x(\bar{p}) > 0.0, \tag{8b}$$

$$x(\pi^-) < 0.5, \tag{8c}$$

where $x = 2P_L^*/\sqrt{s}$. P_L^* is the c.m. longitudinal momentum of the particle and s is the c.m. energy squared of the incident $\bar{p}p$ system. The cuts are based on the x distribution of the well-measured slow positive particles and on CP invariance. The cut on $x(\pi^-)$ resolved some of the mass ambiguities between fast negative tracks and eliminated some events from the sample. The cut (8c) contributes to an observed loss of beam diffractive events that have fast-forward negative pions. However, this is partially compensated by the imposition of CP symmetry in the fitting-efficiency calculation (see below). Only 3.7% of the selected fits have $x(\pi^+) < -0.5$. Upon imposing conditions (8a)–(8c) on events which had kinematic fits for reaction (1), we obtained a unique mass permutation in 94% of the cases. Most of the ambiguities were between high-momentum negative tracks. In case of ambiguities the fit with the lowest χ^2 was chosen. The event sample retained by Eqs. (8) is still not precisely CP symmetric due to the loss of fitted events with two or three tracks forward in the c.m. and also due to the distribution of the background events; see Figs. 1 and 2 for the distribution of x and y^* (y^* = c.m. longitudinal rapidity = $\frac{1}{2}\ln[(E^* + P_L^*)/(E^* - P_L^*)]$, where E^* is the c.m. energy of the particle). The x plots show that the baryons take most of the c.m. momentum in each hemisphere, whereas the pions populate the central region of the x range. On the other hand, the y^* values illustrate the tendency of the pions to travel with one of the baryons. Both distributions exhibit a slight preference of the pion for the direction of the same sign baryon. For reaction (1) the quoted cross sections and partial cross sections are corrected for backgrounds and fitting efficiencies as a function of the kinematic configuration of the events (see below).

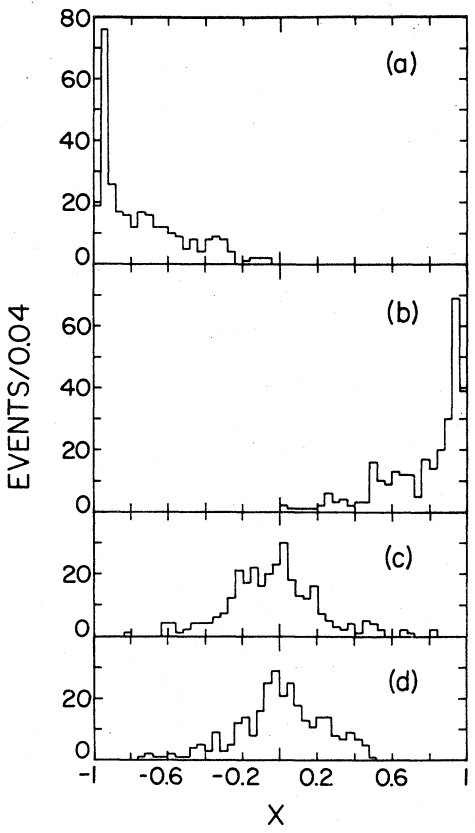

FIG. 1. Feynman-x distributions of the (a) proton, (b) antiproton, (c) π^+, and (d) π^- in the reaction $\bar{p}p \to \bar{p}p\pi^+\pi^-$.

The x cuts imposed on reaction (2) are similar to those of reaction (1):

$$x(p) < 0.325, \tag{9a}$$

$$x(\bar{p}) > -0.325, \tag{9b}$$

$$x(\pi^-) < 0.475. \tag{9c}$$

Since the average momentum of the measured tracks is lower, the apparent CP asymmetry is smaller. Limited statistics preclude x-dependent corrections for reaction (2). Only 6% of the se-

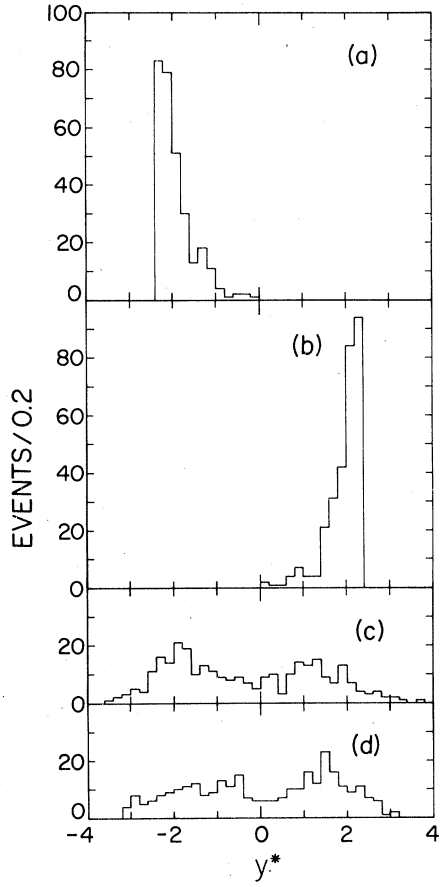

FIG. 2. Center-of-mass longitudinal-rapidity (y^*) distributions of the (a) proton, (b) antiproton, (c) π^+, and (d) π^- in the reaction $\bar{p}p \to \bar{p}p\pi^+\pi^-$.

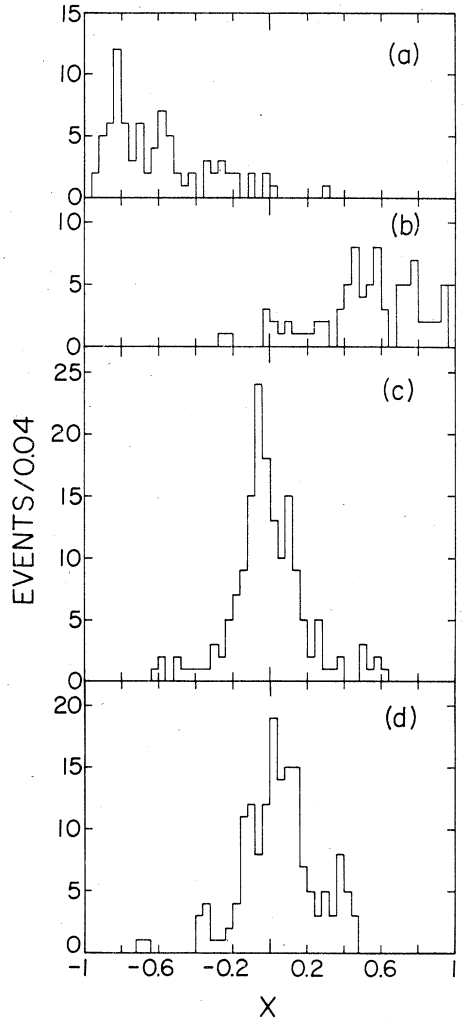

FIG. 3. Feynman-x distributions of the (a) proton, (b) antiproton, (c) π^+, and (d) π^- from the reaction $\bar{p}p \to \bar{p}p2\pi^+2\pi^-$.

lected fits have $x(\pi^+) < -0.475$. After all cuts, 73% of the surviving fitted events had only one mass permutation. For the other 27% of the events the mass permutation with the minimum χ^2 was chosen. See Figs. 3 and 4 for the x and y^* distributions. The baryons are not leading as distinctly in the x distribution as in reaction (1). The cross section to be quoted for reaction (2) is corrected for backgrounds and fitting efficiencies by an amount independent of the kinematic configuration of the events (see below).

The backgrounds were studied by truncating one or two particles from four-constraint four- and six-prong events selected above, and fitting the remaining tracks to the hypotheses $\bar{p}p \to \bar{p}p(k\pi^+)(m\pi^-)$ where k and m are non-negative integers. This procedure was used to estimate the percentage of events with missing neutral mesons, neutral baryons, and/or neutral antibaryons which simulate reactions (1) and (2). To calculate the cross sections of the contaminating channels we relied on a model by von Holt.[2] It was assumed that particle multiplicity distributions are identical for pp interactions and for nonannihilation $\bar{p}p$ interactions. The pp charged particle cross sections at 50 GeV/c needed to evaluate the model were obtained from a global energy-dependent fit discussed in our earlier paper[3] and Ref. 4. The effect of annihilation is neglected due to the small $\bar{p}p$ annihilation cross section into four or six charged particles[3] and the relatively large number of neutral particles produced in annihilation events[5,6] which would tend to prevent fits to the reaction hypotheses(1) and (2). Since we cannot distinguish between π and K mesons, our cross-section estimates for reactions (1) and (2) will include the (probably small) contributions of the corresponding reactions with $\pi^+\pi^-$ pairs being replaced by K^+K^- pairs. Us-

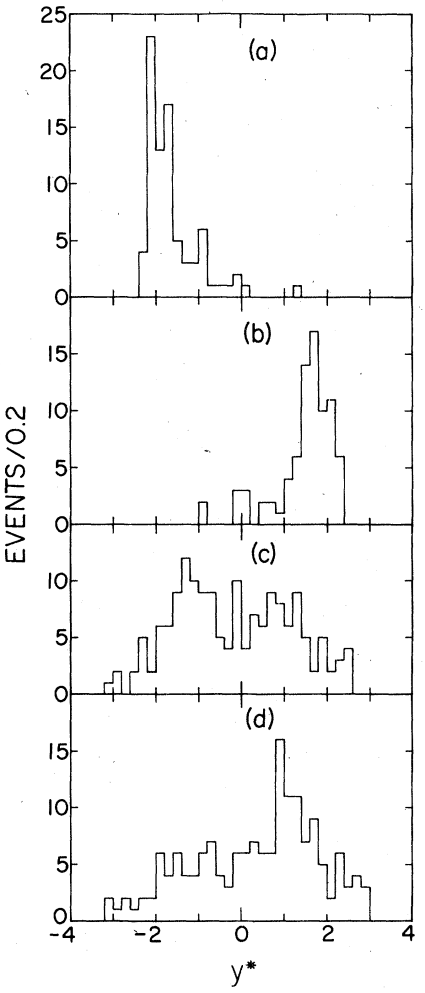

FIG. 4. Center-of-mass longitudinal-rapidity (y^*) distributions of the (a) proton, (b) antiproton, (c) π^+, and (d) π^- from the reaction $\bar{p}p \to \bar{p}p2\pi^+2\pi^-$.

ing the above method, background estimates of (22 ± 8)%, (31 ± 10)%, and (39 ± 14)% of the fitted selected sample were obtained for reaction (1) with zero, one, and two charged pions in the forward c.m. hemisphere, respectively. For reaction (2) an overall background of (53 ± 18)% was calculated.

The number of fits eliminated due to observed associated e^+e^- pairs was consistent with the predicted number of π^0's from the calculated background and the average probability of γ conversion to e^+e^- pairs in the chamber (~2%). In reactions (1) and (2) 4.0 ± 0.9 and 2.2 ± 1.0 γ conversions were predicted and 3 and 1 pairs were found, respectively.

To investigate the fitting efficiency for reaction (1) a random sample of 200 four-prong events was remeasured. Also, events with fits to reaction (1) with $30 < \chi^2 < 50$ were remeasured. New fits from this remeasurement pass obtained with $\chi^2 < 30$ and passing all the above cuts are included in the selected fitted sample. The small random sample of remeasured four-prong events indicated an overall fitting efficiency of (80 ± 10)%. Previously,[1] the fitting efficiency was investigated in the elastic sample by attempting to match with unique downstream wire hits the missing momentum recoiling against the slow positive track. In that case it was found that the major source of elastic fit losses was the uncertainty in the measured momentum of the fast negative track. A 91% elastic fitting efficiency was obtained for the first pass of measurements. A similar procedure was applied to the sample of four-prong events containing one negative and two positive particles in the backward c.m. hemisphere. The slowest negative particle was assumed to be a π^- and if neither of the positive particles was identified as π^+ or p by track ionization density, we took the mass permutation resulting in the smallest missing-mass-squared deviation from the $\bar{p}$ mass squared. When there was a unique wire hit in the first downstream wire chamber, we compared the position of the wire hit with the missing momentum to the p, π^+, and π^- tracks as assigned above. On the basis of these studies the fitting efficiency of events with $p\pi^+\pi^-$ backwards in the c.m. is estimated to be (95 ± 5)%. After background subtraction the efficiency [(64 ± 18)%] is calculated for events with $\bar{p}\pi^-\pi^+$ forward in the center of mass by assuming CP symmetry. For the rest of the four-prong four-constraint-fitted events, the fitting efficiency is taken as the average of the values for events with $p\pi^+\pi^-$ backwards in the c.m. and for events with $\bar{p}\pi^-\pi^+$ forward in the c.m. The fitting efficiencies were then (95 ± 5)%, (79 ± 10)%, and (64 ± 18)% for events with zero, one, and two charged pions forward in the c.m., respectively. The fitting efficiency for reaction (2) was taken to be the same as that of reaction (1) with one forward pion, that is (76 ± 10)%, after taking into account the fact that there were no remeasurements for reaction (2) fits with $30 < \chi^2 < 50$.

After including the above-mentioned corrections as well as corrections for scanning and measuring efficiency,[1] we obtain for reaction (1) a cross section of 1.19 ± 0.19 mb from 295 selected fitted events and for reaction (2) a cross section of 0.33 ± 0.14 mb from 81 selected fitted events. These four-constraint cross sections comprise 11.5 and 3.6% of the four- and six-prong event samples, respectively. In Figs. 5 and 6 these four-constraint four- and six-prong cross sections are compared with results obtained at other energies and with pp interactions. In agreement with earlier results[7] it is

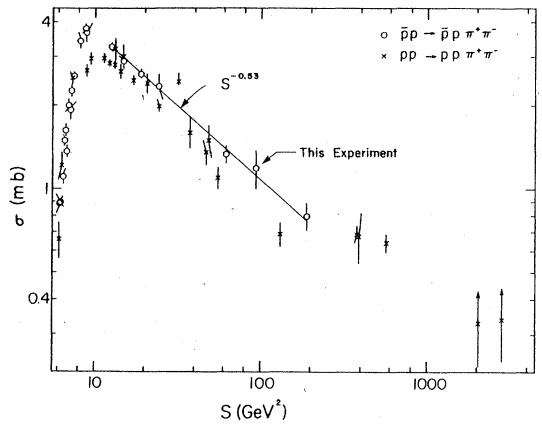

FIG. 5. $\bar{p}p \to \bar{p}p\pi^+\pi^-$ (Ref. 19) and $pp \to pp\pi^+\pi^-$ (Ref. 20) cross sections vs s. The solid line is a fit to $\sigma(\bar{p}p \to \bar{p}p\pi^+\pi^-) \propto s^{-(0.53 \pm 0.03)}$ for $12.6 \leq s \leq 189$ GeV^2.

found that while the four-constraint six-prong cross sections are, within large uncertainties, approximately equal for $\bar{p}p$ and pp interactions, the cross sections of the corresponding four-prong four-constraint reactions are not equal. There is evidence that the difference is not due to diffraction (see below). In addition, the difference is clearly nonannihilation. Specifically, a part of this difference is due (as discussed below) to substantial $\Delta^{++}\bar{\Delta}^{--}$ production via pion exchange in $\bar{p}p$ interactions which has no counterpart in pp four-constraint reactions. One may further speculate that part of the difference is from large interference terms due to exchange amplitudes having opposite sign in the $\bar{p}p$ and pp four-prong nondiffractive reactions. *In any case, this is a clear example where naive subtraction of a pp partial cross section from a similar $\bar{p}p$ partial cross section does not yield an annihilation term.* As was discussed in Ref. 3, there is also further evidence that in low-multiplicity channels the $\bar{p}p - pp$ subtraction procedure does not yield a purely annihilation cross section.

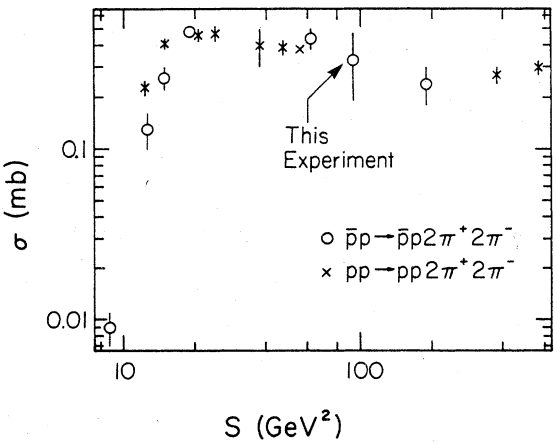

FIG. 6. $\bar{p}p \to \bar{p}p2\pi^+2\pi^-$ (Ref. 21) and $pp \to pp2\pi^+2\pi^-$ (Ref. 22) cross sections vs s.

III. CHARACTERISTICS OF DIFFRACTION AND OF Δ PRODUCTION IN THE REACTION: $\bar{p}p \to \bar{p}p\pi^+\pi^-$

From earlier high-statistics experiments[8,9] it is known that the dominant production mechanisms for reaction (1) can be obtained as kinematic limits of the multiperipheral diagram given in Fig. 7(a) and its CP conjugate. If the rapidity gaps between π^+, π^-, and p are small then we refer to this as target diffractive excitation and we have diagram 7(b). Similarly the CP conjugate of the diagram gives beam diffraction, Fig. 7(c). On the other hand, the reaction $\bar{p}p \to \bar{\Delta}^{--}\Delta^{++}$ is obtained when points 1 and 2 coalesce and points 3 and 4 coalesce to give Fig. 7(d) which proceeds via pion exchange.

To seek evidence for beam or target diffraction, i.e., single-diffractive dissociation, the three-body effective masses $M(p\pi^+\pi^-)$ versus $M(\bar{p}\pi^-\pi^+)$ are plotted in Fig. 8. It is observed that $69 \pm 3\%$ of the events have either $M(p\pi^+\pi^-)$ or $M(\bar{p}\pi^-\pi^+)$ below 2.5 GeV/c^2. Two events having both $M(p\pi^+\pi^-)$ and $M(\bar{p}\pi^-\pi^+)$ below 2.5 GeV/c^2 are excluded. Invoking CP symmetry, we plot in Fig. 9 the combined $M(p\pi^+\pi^-) + M(\bar{p}\pi^-\pi^+)$ distribution. The single-diffraction cross section σ_{SD} of either beam or tar-

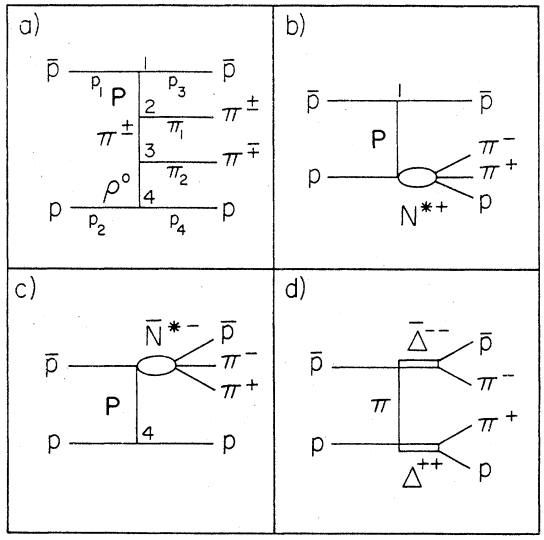

FIG. 7. Reaction diagrams for $\bar{p}p \to \bar{p}p\pi^+\pi^-$: (a) multiperipheral process, (b) target diffraction, (c) beam diffraction, and (d) pion exchange ($\bar{\Delta}^{--}\Delta^{++}$ production). Pomeron exchange indicates the diffractive process in (a), (b), and (c).

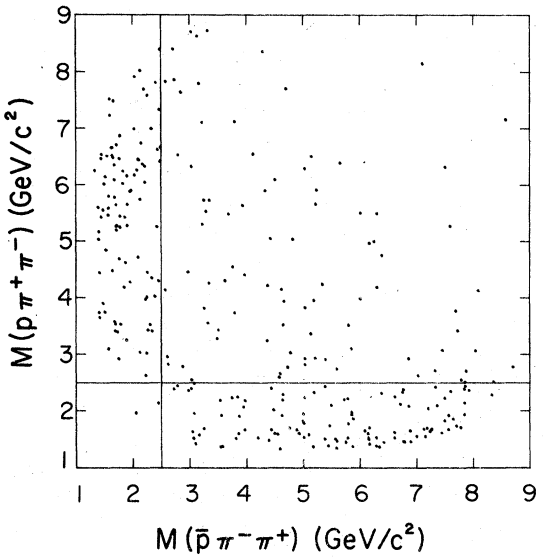

FIG. 8. $M(p\pi^+\pi^-)$ vs $M(\bar{p}\pi^-\pi^+)$ for $\bar{p}p \to \bar{p}p\pi^+\pi^-$. The solid lines indicate the single-diffractive criterion of $M < 2.5$ GeV/c^2.

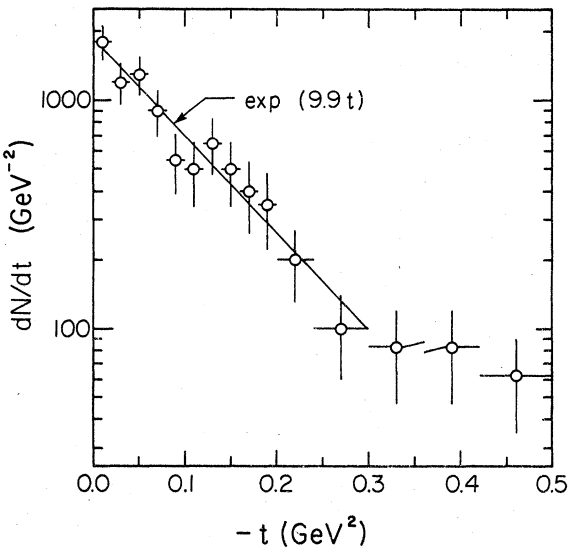

FIG. 10. dN/dt vs $-t$ for beam and target diffraction in $pp \to pp\pi^+\pi^-$ (see text for full explanation). N is the number of selected fitted events. The fit $(2d\sigma_{SD}/dt$ (mb GeV^{-2}) $= (7.5 \pm 1.7)\exp[(9.9 \pm 1.1)t]$, $-t < 0.3$ GeV^2), after having been multiplied by a correction factor for fitting efficiencies and backgrounds, is shown as the solid line.

get, not both, is 0.41 ± 0.06 mb for $M < 2.5$ GeV/c^2. In $(89 \pm 3)\%$ of the events satisfying this definition of single-diffractive dissociation, the particles in the low-mass system are contained in one c.m. hemisphere. After taking into account that we did not require all of the particles in the low-mass system to be in one c.m. hemisphere, we find that σ_{SD} is in excellent agreement with interpolation of $\bar{p}p$ values between 32 and 100 GeV/c laboratory beam momenta and with interpolation of pp values between 12 and 205 GeV/c (see Fig. 5 of Ref. 7). The s dependence of σ_{SD} in this region $[s^{-(0.34\pm0.09)}]$ is less steep than that of reaction (1) as a whole $[s^{-(0.5\sim\ \ .08)}]$ and would be even flatter if the mass cut were enlarged with increasing s in order to include the increasingly massive diffractive states.[10,11]

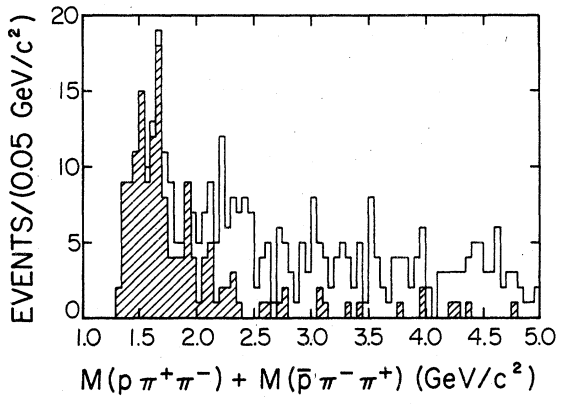

FIG. 9. $M(p\pi^+\pi^-) + M(\bar{p}\pi^-\pi^+)$ from the reaction $\bar{p}p \to \bar{p}p\pi^+\pi^-$. The hatched combinations have $M(p\pi^+) < 1.4$ GeV/c^2 or $M(\bar{p}\pi^-) < 1.4$ GeV/c^2.

In Fig. 10 we show dN/dt vs $-t$ where $t = (p_3 - p_1)^2$ for $M(p\pi^+\pi^-) < 2.5$ GeV/c^2, $t = (p_4 - p_2)^2$ for $M(\bar{p}\pi^-\pi^+) < 2.5$ GeV/c^2, and N is the number of selected fitted events. The characters with numerical subscripts designate four-vectors (see Fig. 7). For $-t < 0.3$ GeV^2, after all corrections the distribution is well described (χ^2/NDF = 4.8/10) by $2d\sigma_{SD}/dt = A \exp(b_{SD}t)$ with $A = 7.5 \pm 1.7$ mb GeV^{-2} and $b_{SD} = 9.9 \pm 1.1$ GeV^{-2}. This differential cross section is multiplied by 2 because the beam and target distributions have been added togehter. The slope b_{SD} is somewhat flatter than the $\bar{p}p$ elastic slope[1,12] of 12.5 ± 0.3 GeV^{-2} found in this experiment. For comparison, the corresponding pp single-diffractive slope[13] is ~10 GeV^{-2} at an incident laboratory momentum of 69 GeV/c.

In Fig. 11 the $M(p\pi^+) + M(\bar{p}\pi^-)$ distribution is presented. A strong $\Delta^{++} + \bar{\Delta}^{--}$ signal is evident. Upon plotting those combinations for which $M(p^\pm\pi^+\pi^-) < 2.5$ GeV/c^2 it is found that the low-mass enhancement "decays" profusely into $\Delta^{++}\pi^-$ or $\bar{\Delta}^{--}\pi^+$ as shown by the hatched portions of Fig. 11. The $p\pi^+\pi^-$ $(\bar{p}\pi^-\pi^+)$ mass combinations which have $M(p\pi^+)$ $(M(\bar{p}\pi^-)) < 1.4$ GeV/c^2 are hatched in Fig. 9.

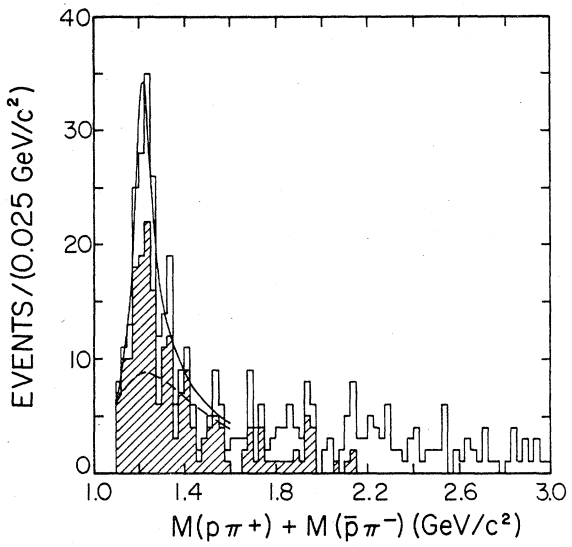

FIG. 11. $M(p\pi^+)+M(\bar{p}\pi^-)$ distribution from $\bar{p}p \to \bar{p}p\pi^+\pi^-$. The hatched portion indicates those combinations which are contained in a diffractive system with $M(p^{\pm}\pi^+\pi^-) < 2.5$ GeV/c^2. The solid line is a Breit-Wigner fit to $\Delta^{++}+\bar{\Delta}^{--}$ in the mass range 1.1–1.6 GeV/c^2 with the mass and width of the resonance fixed at 1232 MeV/c^2 and 115 MeV/c^2, respectively. The dashed line is the nonresonant background piece of the Breit-Wigner fit. Both curves have been corrected for four-constraint fitting efficiencies and for the four-constraint fitted backgrounds fitting as $\bar{p}p \to \bar{p}p\pi^+\pi^-$.

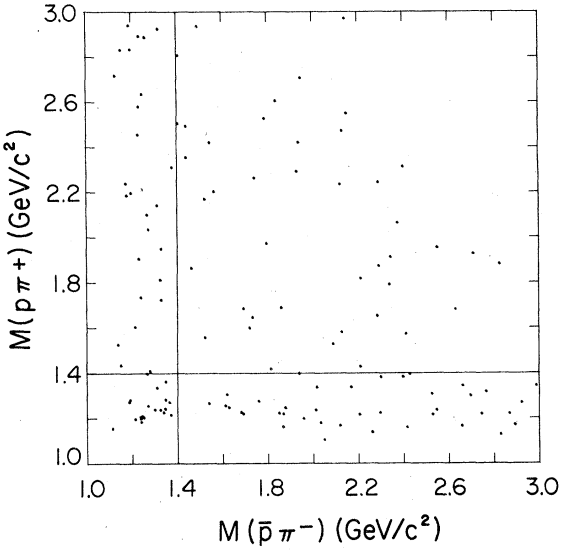

FIG. 12. $M(p\pi^+)$ vs $M(\bar{p}\pi^-)$ in $\bar{p}p \to \bar{p}p\pi^+\pi^-$. The solid lines at 1.4 GeV/c^2 indicate the Δ^{++}, $\bar{\Delta}^{--}$, and $\Delta^{++}\bar{\Delta}^{--}$ regions.

An alternative source of Δ^{++} and $\bar{\Delta}^{--}$ is the reaction (4)

$$\bar{p}p \to \bar{\Delta}^{--}\Delta^{++}$$

via the single-pion-exchange mechanism of Fig. 7(d). In Fig. 12 we present the $M(p\pi^+)$ versus $M(\bar{p}\pi^-)$ scatter plots. An enhancement at the Δ^{++}, $\bar{\Delta}^{--}$ crossing bands is obvious, whereas we do not find a $\Delta^0\bar{\Delta}^0$ signal in the corresponding plot (not shown), a result which is expected from simple isospin arguments.

A clean separation of target diffraction and $\bar{\Delta}^{--}\Delta^{++}$ production can be obtained by plotting the center-of-mass rapidity $y^*(\pi^+)$ versus $y^*(\pi^-)$ as shown in Fig. 13. In the majority of events [(71 ± 3)%] both pions have the same sign of rapidity corresponding predominantly to target or projectile diffraction. There is also a concentration of events with $y^*(\pi^+) < 0$ and $y^*(\pi^-) > 0$, due to reaction (4).

The cross section for reaction (4) is estimated by counting the number of events with $M(p\pi^+)$ and $M(\bar{p}\pi^-) < 1.4$ GeV/c^2. After a subtraction of 6.4 background events extrapolated from adjacent mass bins we find 13.6 $\bar{\Delta}^{--}\Delta^{++}$ events corresponding to 0.054 ± 0.022 mb. The s dependence of the $\bar{\Delta}^{--}\Delta^{++}$ cross section is plotted in Fig. 14 where s is the center-of-mass energy squared. The best fit to the data is $\sigma \propto s^{-(1.57\pm0.17)}$ for $24 < s < 189$ GeV^2. Since the charge-exchange reaction

$$\bar{p}p \to \bar{n}n$$

is also expected to proceed via pion exchange, the energy dependence of the zero-prong cross section is also given in Fig. 14. Of course, the zero-prong cross section can also contain both channels with

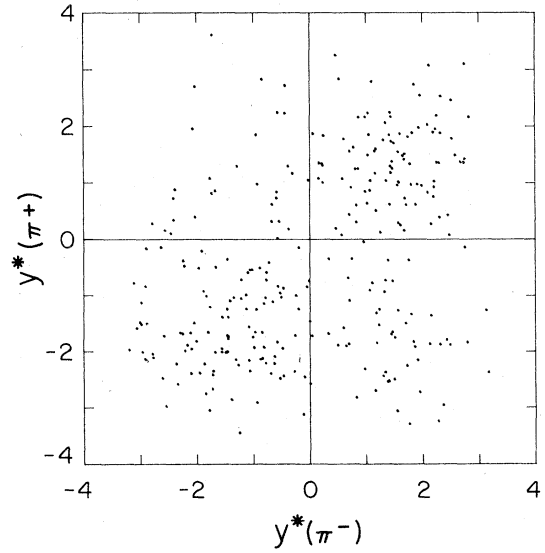

FIG. 13. $y^*(\pi^+)$ vs $y^*(\pi^-)$ in the reaction $\bar{p}p \to \bar{p}p\pi^+\pi^-$.

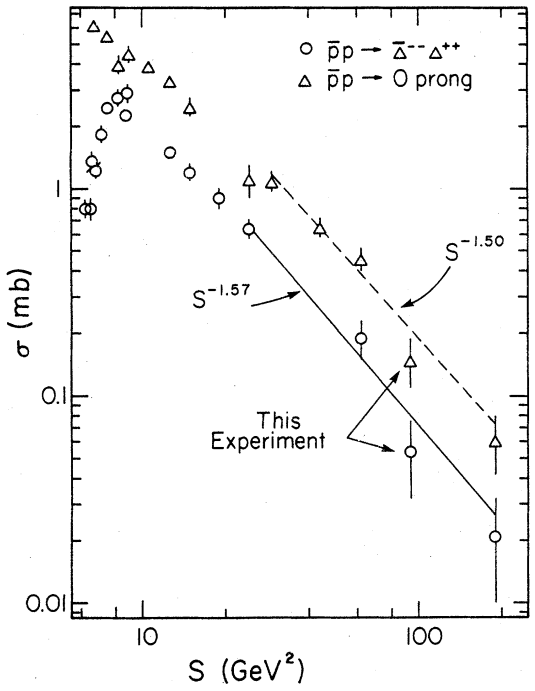

FIG. 14. $\bar{p}p \to \bar{\Delta}^{--}\Delta^{++}$ (Ref. 23) and $\bar{p}p \to 0$ prong (Ref. 24) cross sections vs s. The solid line is a fit to $\sigma(\bar{p}p \to \bar{\Delta}^{--}\Delta^{++}) \propto s^{-(1.57\pm 0.17)}$ for $24 \leq s \leq 189$ GeV^2. The dashed line is a fit to $\sigma(\bar{p}p \to 0 \text{ prong}) \propto s^{-(1.50\pm 0.14)}$ for $30 \leq s \leq 189$ GeV^2.

extra π^0's and also a variety of annihilation channels. Nonetheless, a dependence $s^{-(1.50\pm 0.14)}$ gives a good fit to the data for $29.5 \leq s \leq 189$ GeV^2. Also, it has been found[14] that other meson-exchange cross sections have s^{-n} dependences with $1.5 \lesssim n \lesssim 2.0$ for $s \gtrsim 5$ GeV^2.

In order to calculate the Δ^{++} ($\bar{\Delta}^{--}$) cross sections from reaction (1) the $M(p\pi^+) + M(\bar{p}\pi^-)$ mass distributions have been fitted in the mass range 1.1–1.6 GeV/c^2 by the following form[15,16]:

$$d\sigma(m) = qe^{-bm}(a + cF_{\mathrm{BW}})dm, \tag{10a}$$

where q is the decay momentum in the $p\pi^+$ ($\bar{p}\pi^-$) rest frame, m is the mass of the $p\pi^+$ ($\bar{p}\pi^-$) system, and a, b, c are fitted parameters. F_{BW} is the p-wave Breit-Wigner form

$$F_{\mathrm{BW}} \propto \frac{m}{q}\,\frac{m\Gamma(m)}{(m_0^2 - m^2)^2 + m^2\Gamma^2(m)}, \tag{10b}$$

where

$$\Gamma(m) = \Gamma_0\left(\frac{q}{q_0}\right)^3 \frac{\rho(m)}{\rho(m_0)}, \tag{10c}$$

with

$$\rho(m) = m^{-1}(0.35^2\ \mathrm{GeV}^2 + q^2)^{-1}. \tag{10d}$$

m_0 and Γ_0 are the mass and width of the resonance and are also fitted parameters. Form (10a) assumes that the nonresonant background has the same shape as the effective phase space multiplying the resonance term. A bin width of 25 MeV/c^2 is used in the fit. The average error of $M(p\pi^+)$ is ~5 MeV/c^2 and of $M(\bar{p}\pi^-)$ is ~25 MeV/c^2. Values of m_0 and Γ_0 were obtained in agreement with the standard values[17] of 1232 and 115 MeV/c^2, respectively. They were then fixed for the following analysis. The solid and dashed lines in Fig. 11 show the result of the fit [Eqs. (10)] for the resonance and the nonresonant background term. In each bin a factor has been applied to the fitted form to account for incorrectly chosen four-constraint event backgrounds and four-constraint fitting efficiencies which are discussed in Sec. II. For the following cross-section calculations only the target system was used because of the relatively small contamination which fits kinematically as reaction (1). The resulting cross section for Δ^{++} production is 0.27 ± 0.08 mb. The charge-conjugate system will have an equal cross section. When the corresponding $p\pi^+\pi^-$ mass is restricted to be <2.5 GeV/c^2, a cross section of 0.14 ± 0.06 mb is found for Δ^{++} (or $\bar{\Delta}^{--}$) production in target (or beam) diffraction. These cross sections correspond to 34 ± 15% of the low-mass $p\pi\pi$ (or $\bar{p}\pi\pi$) system.

The $p\pi^-$ and $\bar{p}\pi^+$ mass plots (not shown) do not indicate any significant Δ^0 or $\bar{\Delta}^0$ production. Simple isospin arguments again predict this result. A Breit-Wigner fit gave 0.03 ± 0.02 mb for Δ^0 or $\bar{\Delta}^0$ production, not both. Finally, the $M(\pi^+\pi^-)$ plot (not shown) does not indicate any significant ρ^0 production in reaction (1). A Breit-Wigner fit gave 0.01 ± 0.03 mb.

IV. EXCLUSIVE ANNIHILATION INTO TWO, FOUR, AND SIX CHARGED PIONS

Four-constraint fits to the exclusive annihilation reactions (5), (6), and (7) were attempted on 2564, 2252, and 1455 two-, four-, and six-prong events, respectively, and, as above, a χ^2 cut of 30 was made. Ionization information on slow positive tracks and also all other scan information was required to be consistent with the fits. The fiducial volume cuts allowed secondary track lengths of 15, 20, and 30 cm for reactions (5), (6), and (7), respectively. Where there were ambiguities with nonannihilation four-constraint fits (also having $\chi^2 < 30$) annihilation fits were used in the cross-section upper-limit calculations only if they had the smaller χ^2. Upper limits at 90% C.L. of 0.040, 0.014, and 0.066 mb are determined from 4, 0, and 4 fitted events selected for reactions (5), (6), and (7), respectively. However, extrapolations of the

TABLE I. Summary of $\bar{p}p$ cross sections at 49 GeV/c.

Final state	Cross section (mb)	n [a]	s range [a] (GeV^2)
$\bar{p}p\pi^+\pi^-$	1.19 ±0.19	0.53±0.03	12.6–189
$\bar{p}N^{*+} \to \bar{p}(p\pi^+\pi^-)$ [b,c]	0.41 ±0.06	0.34±0.09 [d]	24–386 [d]
$\bar{p}\Delta^{++}\pi^-(\bar{\Delta}^{--}\Delta^{++}$ excluded) [c]	0.22 ±0.07		
$\bar{p}N^{*+} \to \bar{p}(\Delta^{++}\pi^-)$ [b,c]	0.14 ±0.06		
$\bar{\Delta}^{--}\Delta^{++}$	0.054±0.022	1.57±0.17	24–189
0 prong	0.149±0.039 [e]	1.50±0.14	30–189
$\bar{p}p2\pi^+2\pi^-$	0.33 ±0.14		

[a] The cross section is fitted by a c.m.-energy-squared dependence s^{-n}.
[b] N^{*+} is defined by $M(p\pi^+\pi^-) < 2.5$ GeV/c^2.
[c] The CP-conjugate reaction will have the same cross section.
[d] This value of n is from Ref. 7 where $\bar{p}p$ and pp data were included in the fit.
[e] From Ref. 1.

cross sections of reactions (5)–(7) from low energy[18] predict less than one event for each reaction and the fits selected may well be spurious. Thus the contribution of these four-constraint annihilation channels at 49 GeV/c is found to be negligible.

V. SUMMARY

We have measured the cross sections presented in Table I. Evidence has been given that suggests the reaction $\bar{p}p \to \bar{p}p\pi^+\pi^-$ at 49 GeV/c is dominated by single-diffractive dissociation with the $p\pi^+\pi^-$ or $\bar{p}\pi^-\pi^+$ system having effective mass <2.5 GeV/c^2 in about $\frac{2}{3}$ of the events. The low-mass $p\pi^+\pi^-$ ($\bar{p}\pi^-\pi^+$) system "decays" into $\Delta^{++}\pi^-$ ($\bar{\Delta}^{--}\pi^+$) in (34± 15)% of the single-diffractive events. The single-diffractive slope b_{SD} has been measured as 9.9 ± 1.1 GeV^{-2} which is somewhat smaller than the elastic slope of 12.5 ± 0.3 GeV^{-2}. We found that the exclusive four-prong final state also has a significant branching ratio for $\bar{\Delta}^{--}\Delta^{++}$ production which proceeds via pion exchange as evidenced by the s dependence of the cross section. That is, both the $\bar{\Delta}^{--}\Delta^{++}$ and zero-prong cross sections have $\sim s^{-1.5}$ dependences. At 49 GeV/c no low-mass enhancements were observed for $p2\pi$ or $p4\pi$ systems in the reaction $\bar{p}p \to \bar{p}p2\pi^+2\pi^-$. Exclusive annihilation into two, four, and six charged pions is negligible at 49 GeV/c at the present statistical level.

ACKNOWLEDGMENTS

We would like to thank J. Bishop, J. Brau, R. DeBonte, T. Handler, D. H. Miller, A. Napier, R. Stefansky, L. Stutte, D. Theriot, F. Turkot, R. Walker, R. B. Willmann, and R. K. Yamamoto for their technical help in running and analyzing the $\bar{p}p$ experiment. We also thank the Hybrid bubble-chamber collaboration for the use of their facility. This research was supported in part by the United States Department of Energy.

[1] D. E. Zissa *et al.*, Phys. Rev. D 21, 3059 (1980).
[2] K. von Holt *et al.*, Nucl. Phys. B103, 221 (1976).
[3] R. M. Robertson *et al.*, Phys. Rev. D 21, 3064 (1980).
[4] Y. Tomozawa, Phys. Rev. D 8, 2138 (1973); 8, 2319 (1973).
[5] P. S. Gregory *et al.*, Nucl. Phys. B119, 60 (1977).
[6] D. R. Ward *et al.*, Phys. Lett. 62B, 237 (1976); R. Raja *et al.*, Phys. Rev. D 15, 627 (1977).
[7] C. P. Bust *et al.*, Nucl. Phys. B140, 409 (1978).
[8] E. W. Anderson *et al.*, Lett. Nuovo Cimento 11, 491 (1974).
[9] I. Borecka *et al.*, Nuovo Cimento 5A, 19 (1971).
[10] W. R. Frazer *et al.*, Rev. Mod. Phys. 44, 284 (1972); M. Derrick, Report No. ANL-HEP-CP-75-52, 1975 (unpublished).
[11] V. E. Barnes, in *Proceedings of the IV European Antiproton Conference, Strasbourg, France, 1978* edited by A. Fridman (Editions du Centre National de la Recherche Scientifique, Paris, 1979), Vol. 1, p. 351.
[12] Here, the $d\sigma_{el}/dt \propto \exp[-B\,|t|+C\,|t|^2]$ fit with C fixed at zero has been used from Ref. 1. b_{SD} is evaluated without a $|t|^2$ dependence and the $|t|^2$ dependence in $d\sigma_{el}/dt$ from Ref. 1 is consistent with zero.
[13] D. Denegri *et al.*, Nucl. Phys. B98, 189 (1975).
[14] D. R. O. Morrison, Phys. Lett. 22, 528 (1966).
[15] J. D. Jackson, Nuovo Cimento 34, 1644 (1964).
[16] J. Bartke *et al.*, Nucl. Phys. B137, 189 (1978).
[17] C. Bricman *et al.*, Phys. Lett. 75B, 1 (1978).

[18]E. Bracci *et al.*, Report No. CERN/HERA 73-1 (unpublished).
[19]$\bar{p}p \to \bar{p}p\pi^+\pi^-$, 2.15 → 12 GeV/$c$: Ch. Walck *et al.*, Nucl. Phys. B100, 61 (1975); 32 GeV/c: M. A. Jabiol *et al.*, *ibid.* B127, 365 (1977); 100 GeV/c: C. P. Bust *et al.*, *ibid.* B140, 409 (1978).
[20]$pp \to pp\pi^+\pi^-$, 2.11 → 28.5 GeV/c: E. Bracci *et al.*, Report No. CERN HERA 73-1, 1973 (unpublished); 12 and 24 GeV/c: U. Idschok *et al.*, Nucl. Phys. B53, 282 (1973); 69 GeV/c: D. Denegri *et al.*, *ibid.* B98, 189 (1975); 200 and 300 GeV/c: J. Whitmore, Phys. Rep. 27C, 187 (1976); 205 GeV/c: M. Derrick *et al.*, Phys. Rev. D 9, 1215 (1974); 1080 and 1500 GeV/c: R. Webb *et al.*, Phys. Lett. 55B, 331 (1975).
[21]$\bar{p}p \to \bar{p}p2\pi^+2\pi^-$, 3.6 GeV/$c$: J. Bartke, Report No. CERN 74-18, 172, 1974 (unpublished); 5.7 GeV/c: K. Böckmann *et al.*, Nuovo Cimento 42A, 954 (1966): 6.9 GeV/c: T. Ferbel *et al.*, Phys. Rev. 173, 1307 (1968); 9.1 GeV/c: P. S. Gregory *et al.*, Nucl. Phys. B119, 60 (1977); 32 GeV/c: M. A. Jabiol *et al.*, *ibid.* B127, 365 (1977); 100 GeV/c: C. P. Bust *et al.*, *ibid.* B140, 409 (1978).
[22]$pp \to pp2\pi^+2\pi^-$, 5.5 → 28.5 GeV/c: E. Bracci *et al.*, Report No. CERN/HERA 73-1, 1973 (unpublished); 12 and 24 GeV/c: V. Blobel *et al.*, Nucl. Phys. B111, 397 (1976); 200 and 300 GeV/c: J. Whitmore, Phys. Rep. 27C, 187 (1976).
[23]$\bar{p}p \to \bar{\Delta}^{--}\Delta^{++}$, 2.2 → 12 GeV/$c$: Ch. Walck *et al.*, Nucl. Phys. B100, 61 (1975); 32 GeV/c: M. A. Jabiol *et al.*, *ibid.* B127, 365 (1977); 100 GeV/c: C. P. Bust *et al.*, *ibid.* B140, 409 (1978).
[24]$\bar{p}p \to 0$ prong: Ref. 1 and references therein.